A meshless method based on Point Interpolation Method (PIM) for the space fractional diffusion equation

Q. Liu [a,e], F. Liu [b], Y.T. Gu [c], P. Zhuang [a,e], J. Chen [d], I. Turner [b]

[a] *School of Mathematical Sciences, Xiamen University, Xiamen, Fujian, China*

[b] *School of Mathematical Sciences, Queensland University of Technology, GPO Box 2434, Brisbane, Qld. 4001, Australia, email:f.liu@qut.edu.au*

[c] *School of Chemistry, Physics and Mechanical Engineering, Queensland University of Technology, GPO Box 2434, Brisbane, Qld. 4001, Australia*

[d] *School of Sciences, Jimei University, Xiamen, Fujian, China*

[e] *Fujian Provincial Key Laboratory of Mathematical Modeling and High-Performance Scientific Computation, Xiamen University, Xiamen 361005, China*

Abstract

This paper aims to develop a meshless approach based on the Point Interpolation Method (PIM) for numerical simulation of a space fractional diffusion equation. Two fully-discrete schemes for the one-dimensional space fractional diffusion equation are obtained by using the PIM and the strong-forms of the space diffusion equation. Numerical examples with different nodal distributions are studied to validate and investigate the accuracy and efficiency of the newly developed meshless approach.

Key words: fractional diffusion equation meshless approach point Interpolation Method numerical simulation
PACS: 02.30Jr, 02.60.Cb, 02.70.-c

1 Introduction

In the last decades fractional differential equations have played a very important role in various fields such as mechanics, signal processing, chemistry, electricity and economics. There is a growing realization that relaxation and diffusion phenomena in complex materials cannot be expressed simply in terms

of a sum of exponential decays, each characterized by a single relaxation time or rate.

A physical-mathematical approach to anomalous diffusion may be based on generalized partial differential equations (PDEs) containing derivatives of fractional order in space, or time, or space-time. Consequently many references discussed the analytical and numerical solutions for space, time, and space-time fractional partial differential equations (FPDEs) [1–5]. For space fractional differential equations, most researchers considered the Finite Difference Method (FDM) to discretise the space derivative. Liu et al. [6,7] proposed a computationally effective method of lines. They transformed the space fractional partial differential equation into a system of ordinary differential equations (Method of Lines) that was then solved using backward differentiation formulae. Meerschaert and Tadjeran [8] developed finite difference approximations for fractional advection-dispersion flow equations. Meerschaert et al. [9] derived practical numerical methods to solve two-dimensional fractional dispersion equations with variable coefficients on a finite domain and obtained first order accuracy in space and time. Liu et al. [10] discussed an approximation of the Lévy-Feller advection-dispersion process by a random walk and finite difference method. Zhuang et al. [11] proposed a new implicit numerical method and two solution techniques to improve its convergence order for solving an anomalous subdiffusion equation. Liu et al. [12] presented the numerical simulation for the 3D seepage flow with fractional derivatives in porous media. Sun et al. [13] studied heat and moisture transport through porous textile materials and proposed an uncoupled finite difference method with a semi-implicit Euler scheme in time for the solution of this system. They proved the existence and uniqueness of the solution of the finite difference system. Bolster et. al proved a product rule for vector fractional derivatives using Fourier transforms [14]. Currently, the FDM is one of dominant numerical methods for solving FPDEs and some high-order finite difference methods for fractional partial differential equations attract increasing interests [15–18]. Some researchers considered the Finite Element Method (FEM) or Spectral Method to handle the space derivative. However both FDM and FEM depend on pre-defined grids/meshes which will lead to difficulties when solving many complex problems with irregular field domains.

More recently, many researchers have developed a group of meshless (or meshfree) methods and successfully applied these meshless methods to many fields of computational engineering and science [19,20]. These meshless methods have demonstrated distinguished advantages. First, meshless methods do not use a mesh for the field approximation. Second, an adaptive analysis is easily achievable by a meshless method. Third, the meshless methods are usually more accurate than FDM and FEM because of the use of higher order meshless trial functions. As a result of these unique advantages, meshless methods have good potential for the simulation of FPDE. Nowadays, some works were

reported to handle fractional partial differential equations by the meshless techniques. Chen et al. [21] used the Kansa method for fractional diffusion equations. Gu et al. [22] developed a meshless formulation for the non-linear anomalous sub-diffusion equation and investigated implicit meshless approaches based on radial basis function (RBF) and the moving least squares (MLS) [23,24] to simulate numerically two time fractional diffusion equations. Their results are very encouraged. However, employing meshless methods to the numerical simulation of FPDEs is still limited to time fractional partial differential equation. To the authors best knowledge, no reference has been seen to his point for solving the space fractional differential equation with a meshless method .

In this paper we consider the following one-dimensional space fractional diffusion equation:

$$\frac{\partial u(x,t)}{\partial t} = \kappa \frac{\partial^\alpha u(x,t)}{\partial x^\alpha} + f(x,t), \qquad x \in [0,L],\ 0 < t < T \tag{1}$$

with zero Dirichlet boundary condition

$$\begin{cases} u(0,t) = 0 \\ u(L,t) = 0 \end{cases},\ 0 < t < T \tag{2}$$

and initial condition

$$u(x,0) = \omega(x),\ x \in [0,L] \tag{3}$$

where $\frac{\partial^\alpha}{\partial x^\alpha}$ denotes the Riemman-Liouvile fractional derivative of order $\alpha (1 < \alpha < 2)$ with respect to the variable x, which is defined by [25] as:

$$\frac{\partial^\alpha u(x,t)}{\partial x^\alpha} = \frac{1}{\Gamma(2-\alpha)} \frac{\partial^2}{\partial x^2} \int_0^x \frac{u(\xi,t)}{(x-\xi)^{\alpha-1}} d\xi$$

and $\Gamma(\cdot)$ is the gamma function. In this paper we suppose that the solution of the space fractional differential equation (1-3) satisfies $u(x,\cdot) \in C^2[(0,T)]$.

The objective of this paper is to develop a new meshless approach based on the meshless Point Interpolation Method (PIM) for the spatial discretization of space FPDEs. In Section 2, the governing equation of the space FPDE is given. In Section 3, the PIM is briefly discussed. In Section 4 two full-schemes of the space fractional differential equation with one-order accuracy or two-order accuracy for time are proposed. Section 5 discusses numerical results to testify our approaches. The performance of the newly developed meshless

approaches for space fractional differential equation is investigated. Finally Section 6 presents the main conclusions of the work.

2 Meshless methods for space fractional differential equation

2.1 Construction of the PIM meshless shape function

Consider an unknown scalar function of a field variable $u(x)$ in domain $[0, L]$. The PIM interpolation [19] of $u(x)$ is defined at x as

$$u(x) = \sum_{j=1}^{m} p_j(x)a_j = \{p_1(x)\ p_2(x)\ \cdots\ p_m(x)\} \begin{Bmatrix} a_1 \\ a_2 \\ \vdots \\ a_m \end{Bmatrix} = \mathbf{p}^{\mathrm{T}}(x)\mathbf{a}, \tag{4}$$

where $p_i(x)$ is the given monomial of the spatial coordinate, m is the number of the monomials and a_i is the coefficient of $p_i(x)$ to be confirmed, which will be given in (12) later. The one-dimensional complete polynomial of order p can be represented by the following form

$$\mathbf{p}^{\mathrm{T}}(x) = \{1\ x\ x^2\ \cdots\ x^p\} \tag{5}$$

and the number of basis functions satisfies $m = p+1$. To solve for the coefficient a_i in (4), a local support domain of the point x should be considered, which includes n nodes enclosing the point x. In the traditional PIM, the number of nodes selected in the local support domain always equals to the number m of basis functions, i.e. $n = m$. In Equation (4), the coefficients a_i can be obtained by letting $u(x)$ equal to the real values on the n nodes, i.e.

$$\begin{aligned}
u_1 &= \sum_{i=1}^{m} a_i p_i(x_1) = a_1 + a_2x_1 + a_2x_1^2 + \cdots + a_mx_1^p \\
u_2 &= \sum_{i=1}^{m} a_i p_i(x_2) = a_1 + a_2x_2 + a_2x_2^2 + \cdots + a_mx_2^p \\
&\vdots \\
u_n &= \sum_{i=1}^{m} a_i p_i(x_n) = a_1 + a_2x_n + a_2x_n^2 + \cdots + a_mx_n^p
\end{aligned}$$

The above formula can be written in the following matrix form:

$$\mathbf{U}_s = \mathbf{P}_m\mathbf{a} \tag{6}$$

where $\mathbf{U}_s = (u_1\ u_2\ \cdots\ u_n)^{\mathrm{T}}$ is the vector of function values on the nodes, $\mathbf{a} = (a_1\ a_2\ \cdots\ a_m)^{\mathbf{T}}$ is the vector of unknown coefficients, and

$$\mathbf{P}_m = \begin{bmatrix} 1 & x_1 & x_1^2 & \cdots & x_1^p \\ 1 & x_2 & x_2^2 & \cdots & x_2^p \\ \vdots & \vdots & \vdots & \ddots & \vdots \\ 1 & x_n & x_n^2 & \cdots & x_n^p \end{bmatrix}$$

is the so called moment matrix. Because $n = m$ in PIM, the matrix $\mathbf{P}_m$ is square with dimensions $n \times n$ or $m \times m$.

Solving equation (6), the coefficient vector $\mathbf{a}$ to be determined

$$\mathbf{a} = \mathbf{P}_m^{-1}\mathbf{U}_s. \tag{7}$$

It should be noted here that the coefficients $\mathbf{a}_i$ are constants for the point x. Because if the n interpolation nodes are unchanged, even if the interpolation point is changed, the matrix $\mathbf{P}_m$ determined by the n field nodes is a constant matrix.

Substituting (7) into (4) and noting $n = m$, it can be obtained that

$$u(x) = \mathbf{p}^{\mathrm{T}}(x)\mathbf{P}_m^{-1}\mathbf{U}_s = \sum_{i=1}^{n} \phi_i(x)u_i = \Phi^{\mathrm{T}}(x)\mathbf{U}_s,$$

where $\Phi(x)$ is the vector of shape functions defined by

$$\Phi^{\mathrm{T}}(x) = \mathbf{p}^{\mathrm{T}}(x)\mathbf{P}_m^{-1} = (\phi_1(x)\ \phi_2(x)\ \cdots\ \phi_n(x))^{\mathrm{T}} \tag{8}$$

The derivative of the shape functions of order l (l being a positive integer number or positive real number) can be easily obtained

$$\Phi^{(\alpha)}(x) = \begin{pmatrix} \phi_1^{(\alpha)}(x) \\ \phi_2^{(\alpha)}(x) \\ \vdots \\ \phi_n^{(\alpha)}(x) \end{pmatrix} = \frac{\partial^\alpha \mathbf{p}^{\mathrm{T}}(x)}{\partial x^\alpha}\mathbf{P}_m^{-1},$$

where $\phi_i^{(\alpha)}(x)$ means shape function $\phi_i(x)$s Riemman-Liouville fractional derivative of order α when α is a positive real number. It has been proven that the

PIM shape functions given in Equation (8) satisfy the Kronecker delta condition [19], which makes it easy to enforce the Dirichlet boundary conditions in the meshless method based on the PIM shape functions.

2.2 Meshless approaches

Firstly the problem domain is discretized by properly distributed field nodes. The PIM shape functions obtained in (8) are used to approximate $u(x,t)$. Assume that there are $M+1$ field nodes $x_0 < x_1 < \cdots < x_M$, including $M-1$ internal (domain) nodes and two boundary nodes. Suppose that $\{x_l, l = i_1, i_2, \cdots, i_n\}$ are the nodes selected in the support domain of x_i to construct PIM shape functions, and $\mathbf{D}_i = \{i_1, k_2, \cdots, i_n\}$. Denoting $u_i(t) = u(x_i,t), f_i(t) = f(x_i,t)$ and $\frac{\partial^\alpha u_i(t)}{\partial x^\alpha} = \frac{1}{\Gamma(2-\alpha)}\left[\frac{\partial^2}{\partial x^2}\int\limits_0^x \frac{u(\xi,t)}{(x-\xi)^{\alpha-1}}d\xi\right]\Big|_{x=x_i}$, the following $M+1$ equations are satisfied,

$$\begin{cases} \frac{\partial u_i(t)}{\partial t} = \kappa \frac{\partial^\alpha u_i(t)}{\partial x^\alpha} + f_i(t),\ i = 1, 2, \cdots, M-1 \\ u_0(t) = 0, \\ u_M(t) = 0, \end{cases}$$

where $\frac{\partial^\alpha u_j(t)}{\partial x^\alpha} = \sum\limits_{i \in \mathbf{D}_i} u_i(t)\Phi_i^{(\alpha)}(x_j)$. Because PIM shape functions given in Equation (8) satisfy the Kronecker delta condition, then $\sum\limits_{i \in \mathbf{D}_i} u_i(t)\Phi_i(x_j) = u_j(t)$.

3 Two fully-discrete schemes for time discretization

We discretize time by time instants as follows

$$t_n = n\tau,\ n = 0, 1, 2, \cdots, N,\ \tau = \frac{T}{N},$$

where τ is the time step, and construct two full-discrete schemes for the space fractional differential equation (1) with boundary conditions (2) and initial condition (3).

3.1 Scheme 1: first-order accuracy in time

Let u_j^n be the approximation for $u(x_i, t_n)$. Then applying the first difference quotient to approximate the time derivative, the following fully-discrete scheme can be obtained

$$u_j^{n+1} - \kappa\tau \sum_{i \in \mathbf{D}_i} u_i^{n+1} \Phi_i^{(\alpha)}(x_j) = u_j^n + \tau f_j^{n+1}, \ j = 1, 2, \cdots, M-1 \tag{9}$$

Using Taylors theorem it can be shown that scheme (9) is first-order accurate in time.

3.2 Scheme 2: second-order accuracy in time

Applying Crank-Nicolson scheme to approximate the time derivative and using Taylor's theorem, the following full-discrete scheme can be obtained

$$\begin{aligned} u_j^{n+1} - \tfrac{\kappa\tau}{2} \sum_{i \in \mathbf{D}_i} u_i^{n+1} \Phi_i^{(\alpha)}(x_j) = u_j^n + \tfrac{\kappa\tau}{2} \sum_{i \in \mathbf{D}_i} u_i^n \Phi_i^{(\alpha)}(x_j) + \tfrac{\tau}{2}(f_j^{n+1} + t_i^n), \\ j = 1, 2, \cdots, M-1 \end{aligned} \tag{10}$$

which is with two-order accuracy for time.

4 Numerical results

The following formula about fractional order calculus of power function [25]:

$${}_aD_t^{\alpha}(t-a)^{\gamma} = \frac{\Gamma(\gamma+1)}{\Gamma(\gamma-\alpha+1)}(t-a)^{\gamma-\alpha}, \ (\alpha < 0, \gamma > -1) \ or \ (0 \le m \le \alpha < m+1, \gamma > m)$$

and the Leibniz rule for the fractional order derivative [25] are used in this section to obtain the following result.

$$\frac{\partial^{\alpha}}{\partial t^{\alpha}}(\phi(t)\psi(t)) = \sum_{k=0}^{\infty} \binom{\alpha}{k} \phi^{(k)}(t) \frac{\partial^{\alpha-k}}{\partial t^{\alpha-k}} \psi(t).$$

4.1 Example 1.

Consider the following fractional differential equation

$$\frac{\partial u(x,t)}{\partial t} = \frac{\partial^{1.85} u(x,t)}{\partial x^{1.85}} + f(x,t),\ x \in [0,1],\ t \in (0,0.8] \tag{11}$$

with boundary conditions

$$\begin{cases} u(0,t) = 0 \\ u(1,t) = 0 \end{cases},\ t \in (0,0.8] \tag{12}$$

and initial condition

$$u(x,0) = 0,\ x \in [0,1] \tag{13}$$

where the source term is $f(x,t) = 3.2t^{2.2}x^{3.2}(1-x)^2 - t^{3.2}[\Gamma(4.2)/\Gamma(2.35)(1-x)^2x^{1.35} - 3.7\Gamma(4.2)/\Gamma(3.35)(1-x)x^{2.35} + 3.7\Gamma(4.2)/\Gamma(4.35)x^{3.35}]$. It can be easily proven that the exact solution for this problem is $u(x,t) = t^{3.2}x^{3.2}(1-x)^2$.

Following error norms are defined as error indicators in this paper

$$\varepsilon_\infty = \max_{1 \le i \le N+1} \left| u_i^{exact} - u_i^{num} \right|,\ \varepsilon_0 = \sqrt{\sum_{i=1}^{N+1} (u_i^{exact} - u_i^{num})^2 / \sum_{i=1}^{N+1} (u_i^{exact})^2},$$

In which e_∞ and e_0 are the error norms for the solution, u_i^{exact} and u_i^{num} are exact and numerical solutions, respectively, for interest point i.

4.1.1 Results for scheme 1

The problem domain $[0,1]$ is firstly discretized by regularly distributed field nodes, i.e. $x_i = ih,\ i = 0,1,2,\cdots,50$. The proposed full-scheme (9) is used to simulate this space fractional differential equation. Table 1 lists the detailed results of the computational errors for different time steps. The convergence rates, R, of the two errors regarding to time steps are also listed in the same table. The convergent rate is calculated as:

$$R_\varepsilon = \frac{\varepsilon(\tau_1)}{\varepsilon(\tau_2)}.$$

Table 1
The error obtained by meshless approach at $t = 0.8$ (Regular nodal distribution)

τ	ε_∞	$R_{\varepsilon\,\max}$	ε_0	$R_{\varepsilon 0}$
0.2	1.289e-3	–	9.783e-2	–
0.1	6.719e-4	1.918	5.082e-2	1.925
0.05	3.368e-4	1.995	2.531e-2	2.008

Table 2
Coordinates for 51 irregular distributed field nodes

0	0.025	0.037	0.06	0.083	0.110	0.127	0.144	0.165	0.178
0.205	0.221	0.247	0.263	0.281	0.310	0.325	0.343	0.361	0.387
0.410	0.422	0.441	0.467	0.476	0.507	0.523	0.542	0.568	0.583
0.610	0.624	0.647	0.662	0.688	0.710	0.723	0.746	0.763	0.782
0.810	0.824	0.842	0.868	0.883	0.910	0.923	0.944	0.963	0.982
1									

Table 3
The error obtained by meshless approach at $t = 0.8$ (Irregular nodal distribution)

τ	ε_∞	$R_{\varepsilon\,\max}$	ε_0	$R_{\varepsilon 0}$
0.2	1.313e-3	–	9.986e-2	–
0.1	6.952e-4	1.889	5.287e-2	1.889
0.05	3.599e-4	1.932	2.727e-2	1.939

From Table 1, it can be seen that the convergenc rates are close to

$$R_\varepsilon = \frac{\varepsilon(\tau_1)}{\varepsilon(\tau_2)} = \frac{\tau_1}{\tau_2}.$$

It can be concluded that the order of convergence in time of the present meshless method is $O(\tau)$, which is in good agreement with the results obtained by the theoretical analysis.

The problem domain $[0, 1]$ is discretized using irregularly distributed field nodes as shown in Table 2 and the proposed full-scheme (9) is used to simulate this space fractional differential equation. Table 3 lists the detailed results of the computational errors for different time steps. The convergence rates, R, of the two errors regarding to time steps are also listed in the same table.

Table 4
The error obtained by meshless approach at $t = 0.8$ (Regular nodal distribution)

τ	ε_∞	$R_{\varepsilon\,\max}$	ε_0	$R_{\varepsilon 0}$
0.4	3.255e-4	–	2.502e-2	–
0.2	7.475e-5	4.355	5.569e-3	4.493
0.1	1.162e-5	6.433	7.777e-4	7.161

4.1.2 Results for scheme 2

The problem domain $[0, 1]$ is firstly discretised by regularly distributed field nodes, i.e. $x_i = ih,\ i = 0, 1, 2, \cdots, 50$. The proposed full-scheme (10) is used to simulate this space fractional differential equation. Table 4 lists the detailed results of computational errors for different time steps. From Table 4, it can be seen that the convergence rates are close to

$$R_\varepsilon = \frac{\varepsilon(\tau_1)}{\varepsilon(\tau_2)} = \left(\frac{\tau_1}{\tau_2}\right)^2.$$

It can be concluded that the order of convergences in time of the present meshless method is $O(\tau^2)$.

The problem domain $[0, 1]$ is discretized using irregularly distributed field nodes as shown in Table 5 and the proposed full-scheme (10) is used to simulate this space fractional differential equation. Table 6 lists the detailed results of the computational errors for different time steps. The convergence rates, R, of the two errors regarding to time steps are also listed in the same table.

4.2 Example 2.

Consider the following fractional differential equation

$$\frac{\partial u(x,t)}{\partial t} = \kappa \frac{\partial^\alpha u(x,t)}{\partial x^\alpha},\ x \in [0, 1],\ t > 0 \tag{14}$$

with boundary conditions

$$\begin{cases} u(0,t) = 0 \\ u(1,t) = 0 \end{cases},\ t > 0 \tag{15}$$

Table 5
Coordinates for 101 irregular distributed field nodes

0	0.011	0.022	0.033	0.044	0.056	0.064	0.073	0.085	0.093
0.102	0.111	0.123	0.131	0.144	0.153	0.166	0.171	0.183	0.197
0.205	0.212	0.221	0.235	0.243	0.256	0.261	0.282	0.288	0.292
0.303	0.311	0.327	0.333	0.341	0.359	0.364	0.371	0.386	0.392
0.407	0.412	0.425	0.431	0.448	0.455	0.461	0.478	0.483	0.493
0.510	0.514	0.521	0.538	0.543	0.552	0.568	0.571	0.585	0.592
0.610	0.617	0.629	0.632	0.644	0.651	0.667	0.672	0.684	0.691
0.708	0.715	0.727	0.733	0.741	0.753	0.768	0.772	0.789	0.792
0.803	0.818	0.822	0.833	0.845	0.857	0.863	0.877	0.883	0.891
0.904	0.914	0.922	0.933	0.946	0.952	0.967	0.978	0.987	0.992
1									

Table 6
The error obtained by meshless approach at $t = 0.8$ (Irregular nodal distribution)

τ	ε_∞	$R_{\varepsilon\,\max}$	ε_0	$R_{\varepsilon 0}$
0.4	3.343e-4	–	2.583e-2	–
0.3	8.440e-5	3.961	6.455e-3	4.002
0.1	2.028e-5	4.162	1.540e-3	4.192

and initial condition

$$u(x,0) = \begin{cases} 1,\ x = 0.5 \\ 0,\ x \neq 0.5 \end{cases} \tag{16}$$

Figure 1 shows the response of the space fractional diffusion equation (14) with boundary and initial conditions (15-16) using the proposed full-discrete scheme (9) for different diffusion coefficients κ. It indicates that the solution decays more quickly while the diffusion coefficient κ increases.

Figure 2 plots the numerical solutions's diffusion behaviour while the time increases.

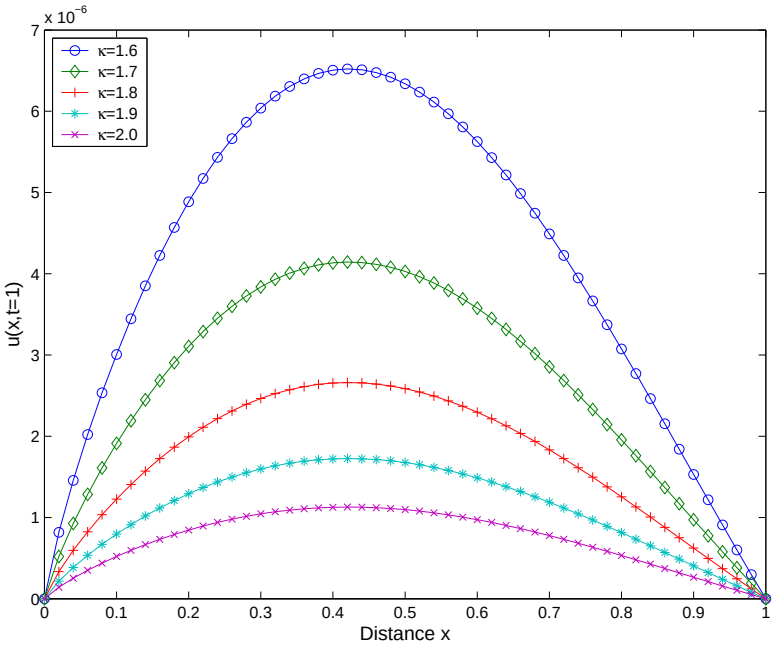

Fig. 1. Numerical solutions for $\alpha = 1.8$ with different diffusion coefficients at $t = 1$.

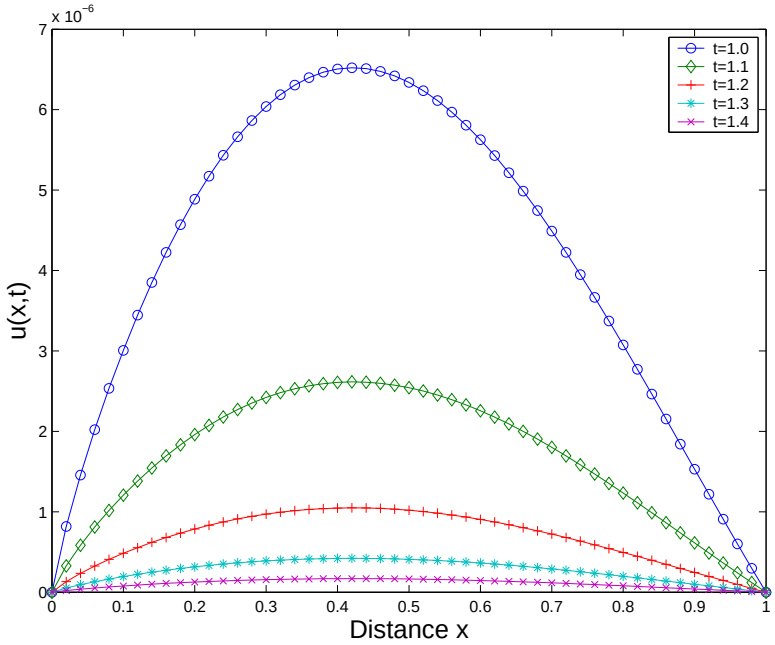

Fig. 2. Numerical solutions for $\alpha = 1.8, \kappa = 1.6$ while the time increases.

In Figure 3, the numerical solutions for different fractional order α are shown. It is well known that the space fractional diffusion equation (1) becomes the traditional diffusion equation when $\alpha = 2$. The fractional derivative (called left fractional derivative in [25]) is not local operator and accumulates the diffusion process from the left end. From Figure 3, the lowest line is not skew as the other lines, which shows that there is not the memory property of

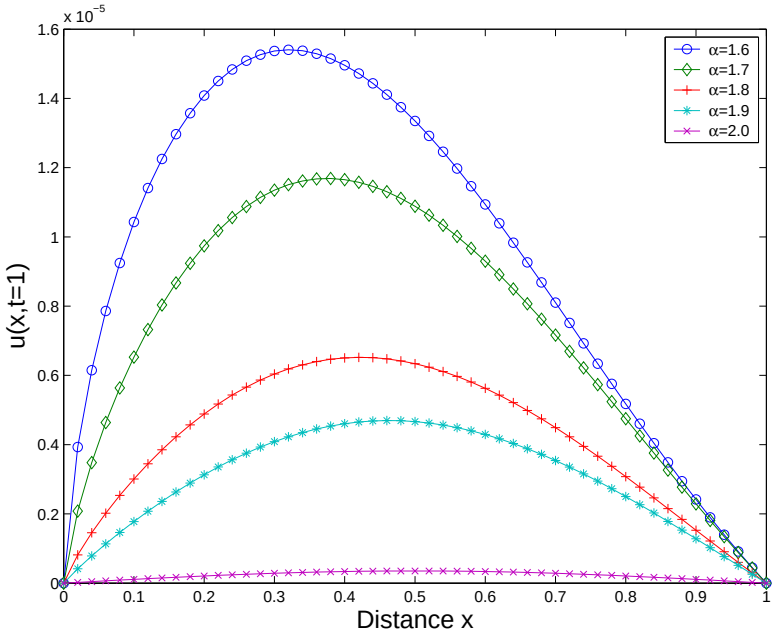

Fig. 3. Numerical solutions for $\kappa = 1.6$ with different fractional order α at $t = 1$.

fractional derivative, instead the locality of integer derivative.

5 Conclusions

This paper aims to develop an implicit PIM meshless approach for the numerical simulation of a space fractional partial differential equation. The first-order accurate and second-order accurate schemes for time are developed and compared. Several numerical examples with different problem domains are used to investigate accuracy and efficiency of the newly developed meshless approaches. Both regular and irregular nodal distributions are employed in the studies. It has been found that the convergence rates of the meshless approach using the first-order and the second-order schemes for time are $O(\tau)$ and $O(\tau^2)$, respectively. It has proven that the newly developed meshless approach is effective for the numerical simulation of the space FPDEs.

6 Acknowledgement:

This work is supported by the ARC Future Fellowship grant (FT100100172), the National Natural Science Foundation of China (Grant No. 11101344), the Natural Science Foundation of Fujian (Grant No. 2013J01021) and the Fundamental Research Funds for the Central Universities (Grant Nos. 2012121001 and 2012121002).

References

[1] V. V. Anh and N. N. Leonenko, Spectral analysis of fractional kinetic equations with random data, J.Stat.Pgys., *104* (2001) 1349-1387.

[2] V. V. Anh and N. N. Leonenko, Harmonic analysis of random fractional diffusion-wave equations. Advanced special functions and related topics in differential equations (Melfi, 2001). Appl. Math. Comput. *141(1)* (2003) 77-85.

[3] A. Saadatmandi and M. Dehghan, A new operational matrix for solving fractional-order differential equations, Computers and Mathematics with Applications, *59* (2010) 1326-1336.

[4] A. Saadatmandi and M. Delghan, A tau approach for solution of the space fractional diffusion equation, Computers and Mathematics with Applications, *62* (2011) 1135-1142.

[5] A. Saadatmandi, M. Dehghan and M. Azizi, The Sinc-Legendre collocation method for a class of The Sinc-Legendre collocation method for a class of fractional convection-diffusion equation with variable coefficients, Communications in Nonlinear Science and Numerical Simulation, *17* (2012) 4125-4136.

[6] F. Liu, V. Anh,I. Turner, and P. Zhuang, Numerical solution for the solute transport in fractal porous media, ANZIAM J. *45(E)* (2004) 461-473.

[7] F. Liu, V. Anh and I. Turner, Numerical solution of the space fractional Fokker-Planck equation, J. Comp. Appl. Math., *166* (2004) 209-219.

[8] M.M. Meerschaert and C. Tadjeran, Finite difference approximations for fractional advection-dispersion flow equations, J. Comp. Appl. Math., *172* (2004) 65-77.

[9] M.M. Meerschaert, H. Scheffler, and C. Tadjeran, J. Comp. Phys., *211* (2006) 249–261.

[10] Q. Liu, F. Liu, I. Turner, and V. Anh, Approximation of the Lvy-Feller advection-dispersion process by random walk and finite difference method, J. Comp. Phys., *222* (2007) 57-70.

[11] P. Zhuang, F. Liu, V. Anh and I. Turner, SIAM J. Numer. Anal., New solution and analytical techniques of the implicit numerical method for the anomalous subdiffusion equation, *46(2)* (2008) 1079-1095.

[12] Q. Liu, F. Liu, I. Turner and V. Anh, IMA J. of Appl. Math., Numerical simulation for the 3D seepage flow with fractional derivatives in porous media, *74* (2009) 201-229.

[13] Wei Sun and Zhi-zhong Sun, Finite difference methods for a nonlinear and strongly coupled heat and moisture transport system in textile materials. Numer. Math., *120(1)* (2012) 153-187.

[14] D. Bolster, M. M. Meerschaert and A. Sikorskii, a Product rule for vector fractional derivatives. Fract. Calc. Appl. Anal., *15(3)* (2012) 463-478.

[15] H. F. Ding, C. P. Li and Y. Q. Chen, High-order Algorithms for Riesz Derivative and Their Applications (I), Abstract and Applied Analysis, *2014* Article ID 653797, 2014.

[16] H. F. Ding, C. P. Li and Y. Q. Chen, High-order Algorithms for Riesz Derivative and Their Applications (II), Journal of Computational Physics, (2014) http://dx.doi.org/10.1016/j.jcp.2014.06.007.

[17] C. P. Li and H.F. Ding, Higher order finite difference method for the reaction and anomalous-diffusion equation, Appl. Math. Model., *38(15-16)* (2014) 3802-3821.

[18] A. Mohebbi, M. Abbaszadeh and M. Dehghan, A high order and unconditionally stable scheme for the modified anomalous fractional subdiffusion equation with a nonlinear source term, Journal of Computational Physics, *240* (2013) 36-48 .

[19] G. R. Liu and Y. T. Gu, Assessment and applications of point interpolation methods for computational mechanics, International Journal for Numerical Methods in Engineering, *59(10)* (2004) 1373-1397.

[20] M. Dehghan and A. Ghesmati, Numerical simulation of two-dimensional sine-Gordon solitons via a local weak meshless technique based on the radial point interpolation method (RPIM), Computer Physics Communications, *181* (2010) 772-786.

[21] W. Chen, L. Ye, and H. Sun, Fractional diffusion equations by the Kansa method, Computers and Mathematics with Applications, *59(5)* (2010) 1614-1620.

[22] Y. T. Gu, P. Zhuang, and F. Liu, An Advanced Implicit Meshless Approach for the Non-Linear Anomalous Subdiffusion Equation, Computer Modeling in Engineering & Sciences, *56(3)* (2010) 303-334.

[23] Q. Liu, Y. T. Gu, P. Zhuang, F. Liu, and Y. Nie, An implicit RBF meshless approach for time fractional diffusion equations, Computational Mechanics, *48* (2010) 1-12.

[24] P. Zhuang, Y. T. Gu, F. Liu, I. Turner, and P. Yarlagadda, International Journal for Numerical Methods in Engineering, Time-dependent fractional advectionCdiffusion equations by an implicit MLS meshless method, *88* (2010) 1346-1362.

[25] I. Podlubny, *Fractional differential equations*, (Academic Press, 1999).